3D numerical simulations in complex near-field geological configurations during the M_W 6.3 L'Aquila earthquake

C. Smerzini, M. Villani, E. Faccioli & R. Paolucci
Department of Structural Engineering, Politecnico di Milano, Italy

SUMMARY:
In this work we illustrate the main results regarding 3D numerical simulations of the M_W 6.3 L'Aquila earthquake on Apr 6th 2009. A 3D linear-elastic numerical model was constructed to propagate up to frequencies of about 2.5 Hz, including a realistic description of the Aterno Valley and of the fault rupture as well. The numerical results turn out to be in satisfactory agreement with the strong ground motion records within the L'Aquila urban area, although some discrepancies are found in the upper Aterno Valley.
To make the synthetic ground motion usable for engineering applications, a hybrid method has been used to combine low frequency waveforms from GeoELSE with high frequency synthetics simulated through stochastic techniques. Displacement and acceleration response spectra of synthetic broadband ground motions were found to be in good agreement with the observations, especially at the stations within the L'Aquila urban centre.

Keywords: spectral element numerical simulations, broadband ground motions, kinematic seismic source

1. INTRODUCTION

A reliable characterization of ground shaking during large damaging earthquakes is of primary relevance for guiding seismic hazard studies at a national scale and for the determination of the seismic demand for design of strategic structures in densely populated urban areas. With the increasing use, on one side, of nonlinear time domain analysis techniques in performance-based earthquake-resistant design of structures and, on the other side, of deterministic scenarios as input motion for the risk assessment of large urban areas (see e.g. Jones et al., 2008), synthesizing reliable seismic ground motion and its spatial distribution at an extended territory has gained major importance for the selection of the proper seismic input.
Despite the increasing number of high quality accelerometric archives worldwide in recent years, the use of natural accelerograms from past earthquakes under similar conditions to that of the design earthquake is hardly feasible from a practical viewpoint. Thanks to the improvement of the numerical tools and to the increase of computational resources, physics-based deterministic modelling of real, or realistic, earthquakes has emerged as a powerful alternative to the use of real earthquake records, for many engineering and seismological applications (Day et al., 2008; Graves et al., 2010; Bielak et al., 2010).
The near-fault conditions, the complex geological setting and the availability of an unprecedented dataset of high quality near fault strong ground motion records make the 2009 M_W 6.3 L'Aquila earthquake a relevant opportunity to check the feasibility and effectiveness of numerical ground motion simulation tools during real earthquakes. The earthquake struck the Abruzzi region in Central Italy, causing about 300 deaths and vast destructions in the town and surroundings of L'Aquila, the medieval capital city of the region with about 80,000 inhabitants. The L'Aquila earthquake represents the third largest event recorded by strong-motion accelerometers in Italy, after the M_W 6.9, 1980, Irpinia and the M_W 6.4, 1976, Friuli earthquakes, but it is for sure the best documented from an instrumental viewpoint.
The main aim of this work is to illustrate the most significant results obtained through 3D numerical

simulations of the L'Aquila mainshock. Numerical simulations have been carried out making use of the Spectral Element Method (SEM) implemented in the numerical code GeoELSE. The computational grid was constructed to accurately propagate frequencies up to 2.5 Hz, including a simplified but realistic 3D model of the Aterno river valley and a kinematic characterization of the seismic source. The comparison between observed and simulated waveforms will be discussed, focusing on the effect of physics-based stochastic variations of kinematic source parameters and the generation of realistic ground shaking maps.
To make the simulated waveforms usable over a broad frequency range of interest for engineering purposes, say up to about 20 Hz, a hybrid scheme (see e.g. recent applications by Graves and Pitarka, 2010; Mai et al., 2010; Ameri et al., 2012) has been applied to generate broadband ground motions, combining Low Frequency (LF) waveforms from GeoELSE (f < 2.5 Hz) with High Frequency (HF) synthetics (f > 3 Hz) from stochastic techniques.

2. THE M_W 6.3 EARTHQUAKE OF APRIL 6TH 2009

In the night of Apr 6th 2009, at 01:32 UTC, a M_W 6.3 earthquake struck the Abruzzi region, causing about 300 deaths and vast destructions in the town and L'Aquila surroundings, with maximum MCS intensities IX-X (Galli et al., 2009).
The earthquake followed a seismic sequence that initiated in October 2008 and culminated with a M_L=4.1 event on March 30th, and the M_L=3.9 event a few hours before the mainshock. The aftershock distribution (Chiarabba et al., 2009), as well as DinSAR analyses (Atzori et al., 2009), geodetic and geological surveys (Anzidei et al., 2009), suggest that this event occurred on the Paganica fault, a 15 km long NW-SE striking (about 150°), SW-dipping structure, that was unknown prior to the L'Aquila earthquake (see superimposed rectangle in Figure 2.1).
Among the several strong motion stations that recorded the earthquake, some were located on the hanging wall of the causative fault at less than 5-6 km from the epicentre, displaying very clear near-field signals with evident static offsets (Ameri et al., 2009).
The main features of the near fault strong motion dataset are listed in Table 2.1: Peak Ground Acceleration (*PGA*) values range from about 0.25-0.35 g in downtown L'Aquila (stations AQK and AQU) to 0.40-0.65 g along the Aterno river array. Horizontal Peak Ground Velocity (*PGV*) recorded at the various stations is fairly similar, ranging from about 20 to 40 cm/s, while remarkable differences are found in the vertical component. Vertical PGV is around 10 cm/s along the Aterno river, while it attains about 25 cm/s at AQK and AQU.

Table 2.1. Main features of the near fault strong motion dataset. The recorded values of horizontal and vertical Peak Ground Acceleration (PGA_h and PGA_v, respectively) and Velocity (PGV_h and PGV_v) are listed. R_e denotes the epicentral distance. The star indicates that the value of V_{S30} (shear wave velocity averaged over the top 30 meters) is not available.

Code Station	Long [°]	Lat [°]	Elev. [m]	R_e [km]	EC8 Soil Type	PGA_h [cm/s^2]	PGA_v [cm/s^2]	PGV_h [cm/s]	PGV_v [cm/s]
AQA	13.339	42.376	693	4.6	B	435.77	466.85	31.77	9.98
AQG	13.337	42.373	721	4.4	B	501.32	266.47	36.3	10.9
AQV	13.344	42.377	692	4.9	B	652.16	540.4	43.5	11.97
AQU	13.402	42.359	729	6	B*	357.31	361.86	36.76	22.83
AQK	13.401	42.345	726	5.7	B	307.33	345.5	30.6	26.04

The epicentral area of the L'Aquila earthquake lies in the upper and middle Aterno valley, which is a typical intermontane Quaternary basin generated by the normal fault extensional tectonic regime that dominates the seismic activity in Central Italy along the Appennines chain. The L'Aquila basin, with its elongated shape along the NW-SE direction, is located between the Gran Sasso mountain and the Monti d'Ocre-Velino-Sirente structural units and extends for several tens of kilometers.
After the 2009 Aquila earthquake sequence, the Department of Civil Defence of Italy (DPC) carried out detailed microzonation studies (MS-AQ Work Group, 2010), that produced the geological map

shown in Figure 2.1. On the map two representative cross-sections, namely M1S2 and M2S4, passing through the historical center of L'Aquila and the upper Aterno Valley, NW of L'Aquila, respectively, are highlighted.
The town of L'Aquila lies on a river terrace, some tens of meters thick, formed by alluvium Quaternary breccias (*megabrecce*), laying on lacustrine sediments, composed mainly of silty and sandy layers and minor gravel beds, the thickness of which reaches its maximum value, around 250 m, in the center of L'Aquila, while it does not exceed 100 m in the upper Aterno River valley, north of L'Aquila (Blumetti et al., 2002). Further details on the microzonation activities performed within the historical L'Aquila city center can be found in Milana et al. (2011).

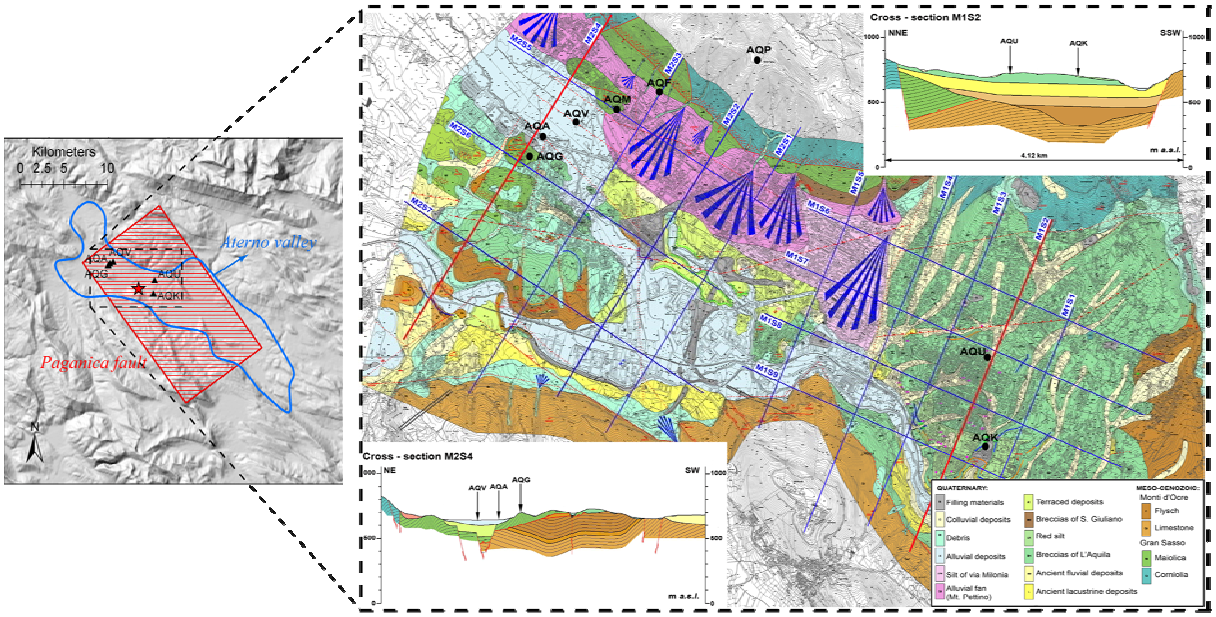

Figure 2.1. Left: Digital Elevation Model (DEM) of the area under study displaying the L'Aquila basin and the Paganica fault. The epicenter of the L'Aquila earthquake is denoted by the superimposed star. Right: geology of the upper and middle Aterno valley after the seismic microzonation studies (adapted from MS-AQ Work Group, 2010): two cross-sections are shown, namely, M1S2, close to L'Aquila center, and M2S4, NW of L'Aquila. The location of the strong motion stations is also highlighted.

3. NUMERICAL SIMULATIONS BY A SPECTRAL ELEMENT CODE

3D numerical simulations of the seismic response of the Aterno Valley during the M_W 6.3 mainshock were performed making use of the SEM implemented in the software package GeoELSE (GeoELastodynamics by Spectral Elements, http://geoelse.stru.polimi.it). The code is designed to perform 2D/3D linear and non linear elastic seismic wave propagation analyses in highly heterogeneous media, exploiting in 3D its implementation in parallel computer architectures. The code, based on the formulation proposed by Faccioli et al. (1997), was jointly developed by the Center for Advanced Research, Studies and Development in Sardinia (CRS4) and by Department of Structural Engineering and of Modelling and Scientific Computing (MOX) of Politecnico of Milano.
A 3D SE model was constructed including the following features:

i) a simplified but realistic 3D model of the Aterno Valley alluvial cover, as inferred from the in-situ investigations described in the previous Section;
ii) a layered deep crustal model for the background geological structure based on preliminary geophysical surveys (Melini and Casarotti, Pers. Comm., 2009);
iii) a suitable kinematic representation of the Paganica fault according to seismic source inversion study of Walters et al. (2009).
iv) a linear visco-elastic material behaviour with quality factor *Q* proportional to frequency.

With reference to point i), as a reasonable balance between the spatially heterogeneous results from the microzonation studies and the practical need to build a computational mesh with reasonable simulation times, a simplified model for the Aterno Valley was defined, considering the submerged bedrock topography, as retrieved from microzonation studies, and an average soil profile, expressed as a function of depth *z* (measured from the topographic surface) as follows:

$$V_S = 500 + 10\sqrt{z} \qquad V_P = \sqrt{3}V_S \qquad \text{[in m/s]}$$
$$\rho = 2000 \qquad \text{[in kg/m}^3\text{]} \qquad (3.1)$$
$$Q_S = 50$$

where V_S and V_P are the S- and P- wave velocity, respectively, ρ denotes the soil density and Q_S is the quality factor for S- waves at the reference frequency of 1 Hz.
As regards the seismic source, GeoELSE features a number of options that makes it suitable for the kinematic modelling of an extended fault model by assigning a realistic distribution of co-seismic slip.
The finite fault solution of Walters et al. (2009), whose main features are summarized in Table 3.1, has been adopted in GeoELSE. The hypocenter is located at 42.35°N, 13.38°E at a depth of 9.6 km (Cirella et al., 2009). A ramp-type slip time function was assumed as sketched in Figure 3.1. The definition of the source model in GeoELSE has been enriched by defining the kinematic source parameters, such as rise time (τ_R), rupture velocity (V_R) and rake angle (λ), as stochastically correlated spatial fields with physical constraints on the coherence across the fault plane and the correlation with co-seismic slip (Mai and Beroza, 2002). Details of the implementation of such features in GeoELSE can be found in Smerzini and Villani (2012).

Table 3.1. Finite fault solution proposed by Walters et al. (2009) and implemented in the SE numerical model. The hypocenter location is also shown.

Hypocenter		**Focal Depth**	**Length**	**Width**	**Strike**	**Dip**	**Rake**
Long	**Lat**	**[km]**	**[km]**	**[km]**	**[°]**	**[°]**	**[°]**
42.35°N	13.38°E	9.6	20	18.5	144	54	-105

The 3D hexahedral spectral element mesh adopted for the numerical simulations with GeoELSE, including the earthquake source, the horizontally layered crustal geology model and the Aterno Valley, is illustrated in Figure 3.1 The map on the right shows the slip distribution for the kinematic source model of Walters et al. (2009). Note that the numerical grid reproduces the surface topography, as the SEM allows for a natural treatment of the free surface condition.
The mesh consists of 376'831 elements (10'419'640 nodes for Spectral Degree SD = 3), the size of which ranges from a minimum of about 150 m within the quaternary basin up to around 600 m at outcropping bedrock. The mesh was designed to propagate up to about 2.5 Hz. Referring to the simulation with SD = 3, the time step for the explicit second-order finite difference time integration scheme is $\Delta t = 1.0 \cdot 10^{-3}$ s for a total simulated time D = 30 s. The simulations were carried out on a cluster using 64 CPUs in parallel, resulting in a total computer time of about 7 hours for a single simulation.

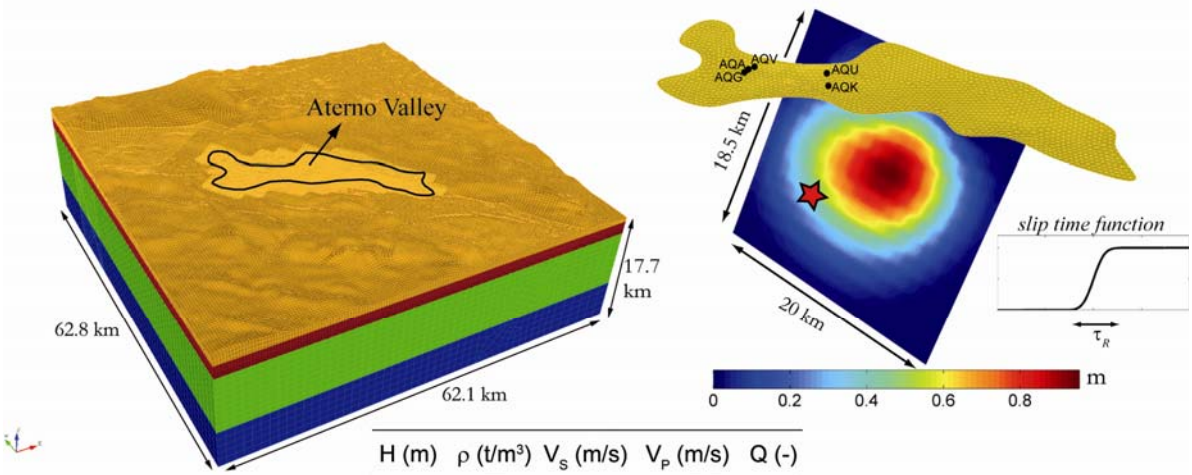

H (m)	ρ (t/m³)	V_S (m/s)	V_P (m/s)	Q (-)
1070*	2.6	1531	3062	100
2000	2.6	2770	4709	200
9000	2.8	3797	7024	300
6650	2.8	3315	6000	300

*beneath AQK

Figure 3.1. 3D hexahedral spectral element mesh adopted for the numerical simulations. The crustal model is horizontally layered, as listed in the superimposed table.

3.1. Results of numerical simulations

Before focusing on the comparison between recorded and simulated waveforms, we now touch on the issue regarding the effect of seismic source heterogeneity on simulated earthquake ground motion. To this end, we illustrate in Figure 3.2 the comparison between the results obtained with a simple source model, referred to as SS hereafter, with those obtained with a complex source model, referred to as CS. For the SS, we have assumed a homogeneous spatial distribution of rise time, rupture velocity and rake angle across the fault plane, with values: τ_R = 0.9 s, V_R = 2.5 km/s, and λ = 255. On the other hand, for the CS, these kinematic parameters are described as correlated stochastic fields with average properties equal to those of the SS. Leaving aside the details regarding the CS, we limit herein to recall that the parameters of such stochastic fields were calibrated to fit as much as possible the information resulting from the seismic source inversion studies. Note that the slip pattern is the same for model SS and CS, as depicted in Figure 3.1 (right map). For comparison purposes, the AQK and AQV recordings are also shown (black line).

It is found that accounting for random heterogeneities in the kinematic source description plays a significant role in exciting HF components of ground motion above 0.7 Hz approximately. Sensitivity analyses with respect to the properties of random source distributions, not shown here for brevity, have highlighted that variations of rise time have the greatest impact on energy at HF, since the rise time acts as a low pass filter with cut-off frequency approximately equal to $1/\tau_R$ (Herrero and Bernard, 1994).

Figure 3.3 illustrates the comparison between the numerical results, obtained for the CS discussed above, and the recorded waveforms, in terms of three component velocity time histories (filtered in the range 0.1-2.5 Hz). The comparison is shown for four strong motion stations, namely, AQK and AQU, within L'Aquila center, AQG and AQV, deployed along the upper Aterno Valley array.

Referring to AQK station, a good agreement between recorded and simulated waveforms is found, in terms of first arrivals, duration and spectral Fourier amplitudes (not shown here for brevity). Similarly, the comparison is satisfactory also for station AQU, although the numerical model tends to underestimate the NS component.

On the other hand, the agreement between simulated and observed signals grows worse for the stations of the Aterno valley array. At AQV and AQG, first arrivals are reasonably well captured by the simulations, especially in the EW and vertical components, but the ground motion amplitudes are

strongly underestimated. Such discrepancies, observed at all the Aterno array stations, are most likely due, on one side, to some rough approximations of the geological model, especially in the northern portion of the valley, and, on the other side, to the kinematic source models, which radiate most energy in the SE direction.

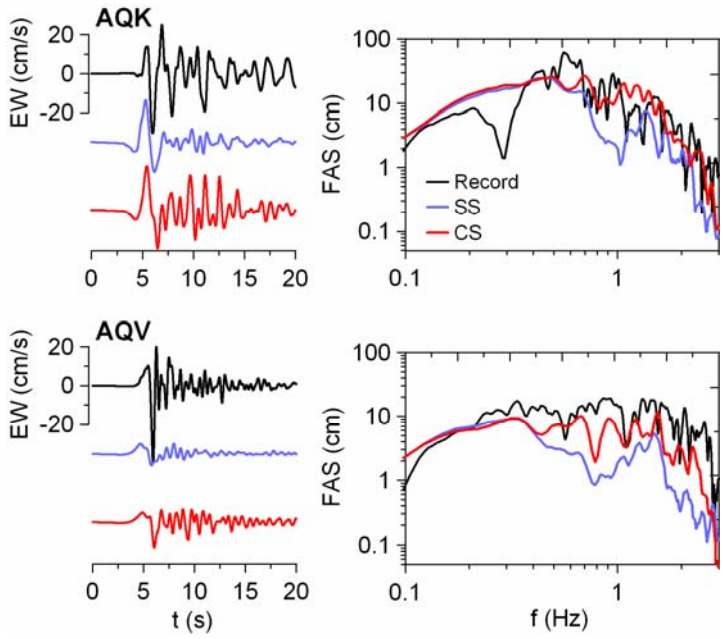

Figure 3.2. Effect of seismic source complexity: comparison between the results obtained with a Simple Source (SS, in blue) and those obtained using a Complex Source (CS, in red) in terms of horizontal (EW component) velocity time histories (left hand side) and corresponding Fourier spectra (right hand side) at AQK (top) and AQV (bottom). Ground motion recordings (black lines) are also displayed for comparison purposes. All data are filtered between 0.1 and 3 Hz.

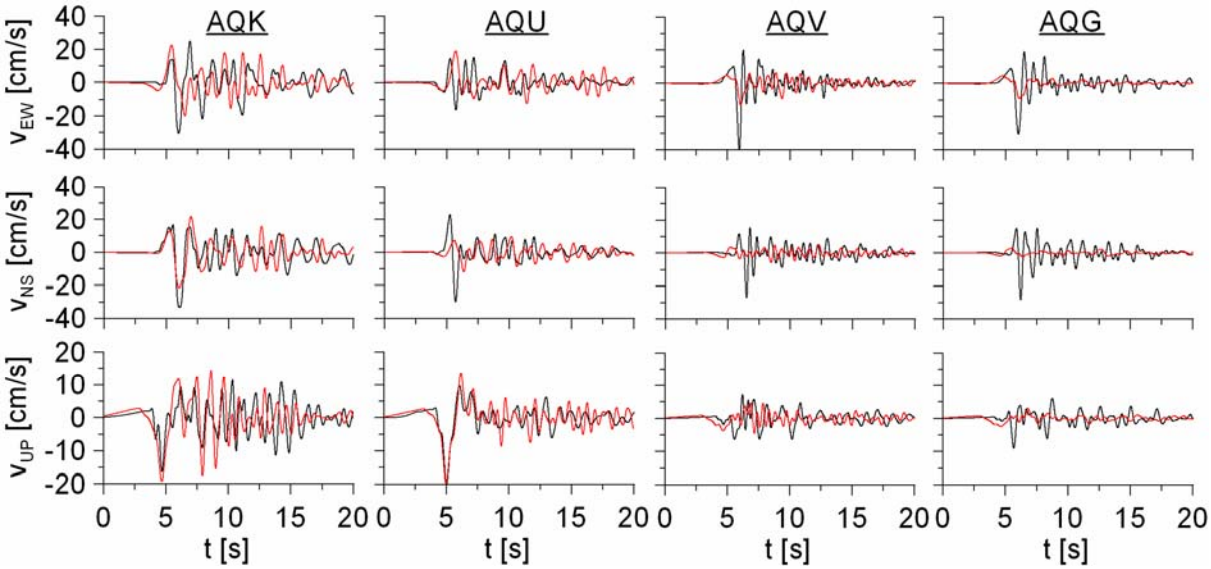

Figure 3.3. Comparison between observed (black) and simulated (red) waveforms in terms of three-component velocity time histories at four strong motion stations, namely, AQK, AQU, AQV, and AQG, in the epicentral area of L'Aquila earthquake.

3D numerical simulations give insights into seismic wave propagation effects, that could not be reproduced by standard 1D and 2D approaches, and make it possible to generate realistic ground shaking maps for future fault rupture scenarios in realistic geological configurations. Figure 3.4

illustrates the comparison between the observed MCS macroseismic intensity field (DMBI Working Group, 2009) and the simulated *PGV* wavefield, computed as geometric mean of horizontal components. It is noted that the simulated *PGV*s are in reasonable agreement with the observed distribution of damage in the epicentral area, pointing out that the numerical simulations are able to reproduce realistic pictures of the spatial distribution of earthquake ground motions at extended territory.

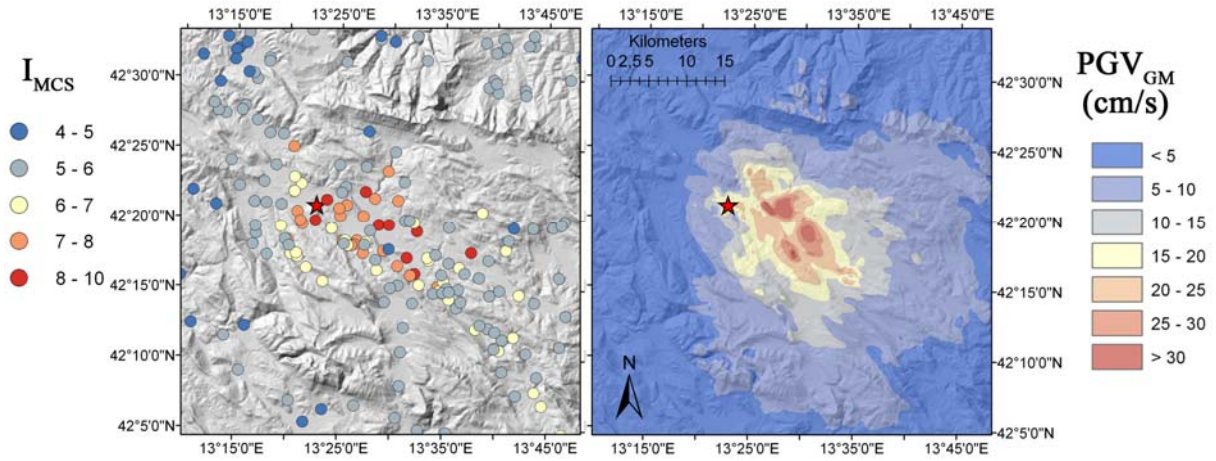

Figure 3.4. Comparison between the observed MCS macroseismic intensity field (left) and the simulated *PGV* wavefield (right). The superimposed star denotes the epicenter location.

4. GENERATION OF BROADBAND WAVEFORMS

The need of ground motion synthetics apt for damage assessment leads us to remove the f_{max} = 2.5 Hz limit of 3D numerical simulations, through the injection of higher frequency components. In this study, the stochastic method of Boore (1983), implemented in the code EXSIM (Motazedian and Atkinson,2005), has been used for the generation of high frequencies synthetics. As a matter of fact, EXSIM features a number of options that make it suitable for the scope of the present work, among which: (i) the possibility to model heterogeneous slip pattern consistent with the 3D SE model; and (ii) modification of ground motion due to local site conditions through simplified 1D amplification functions. The major drawback of the method is that it can not distinguish between the two horizontal ground motion components. To overcome such limitation, twenty stochastic simulations have been performed for generating the EW component and twenty more for the NS one. For all stochastic simulations, the fault model of Walters et al. (2009) was considered.

For each site of interest and for each stochastic realization, broadband (BB) waveforms were generated by combining the LF waveforms from GeoELSE ($f \leq 2.5$ Hz**)** with the HF signals from EXSIM calculations ($f > 3$ Hz) through suitable match filters in the frequency domain. The procedure used to compute BB signals is sketched in Figure 4.1.

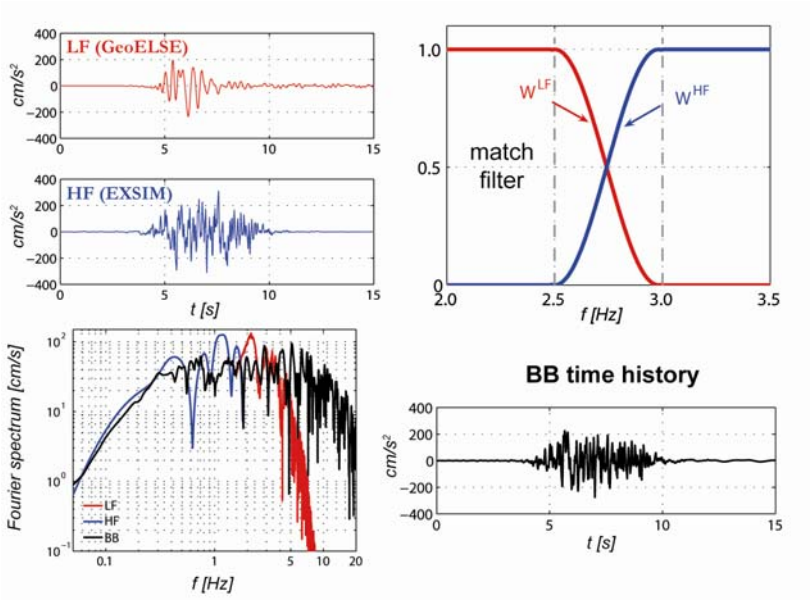

Figure 4.1. Procedure to generate broadband (BB) signals (black lines): combination of LF waveforms from GeoELSE for $f \leq 2.5$ Hz (red) with HF synthetics from EXSIM for $f > 3$ Hz (blue) by applying match filters.

The comparison between the observations (black) and the synthetic median BB waveforms (red) is depicted in Figure 4.2, in terms of pseudo-acceleration PSA (top panel) and displacement SD (bottom panel) response spectra, computed as geometric mean of the horizontal components. Note that the 50th percentile of the BB response spectral ordinates is shown in each plot of Figure 4.2.

It is found that the synthetic BB response spectral ordinates are in good agreement with the observations at long periods, in particular at AQK and AQU stations, where the 3D simulations capture well the significant features of the recorded ground motion. On the other hand, at the same stations, the spectral ordinates for T<0.5 s, contributed by the EXSIM results, are larger than the recorded ones. At AQV, the injection of HF contributions into the 3D deterministic results tends to improve the agreement but the response spectral amplitudes are still lower, by a factor of about 3 in terms of PGA value and of about 1.6 in terms of maximum SD, than the observed ones.

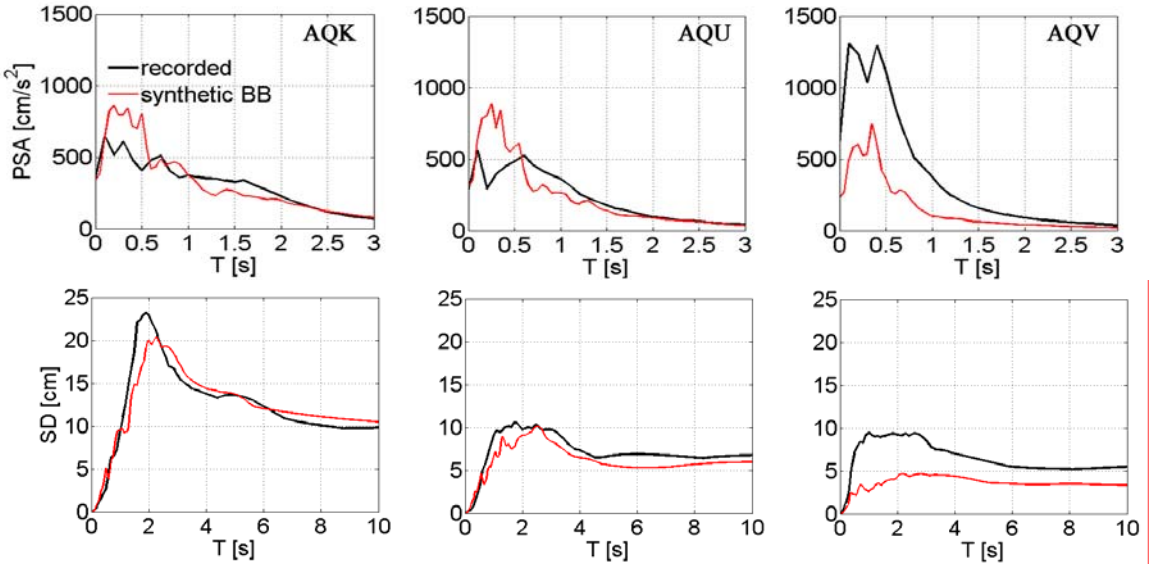

Figure 4.2. Comparison between synthetic broadband (BB) signals (red lines) and observations (black) in terms of pseudo-acceleration (PSA, top panel) and displacement (SD, bottom panel) response spectra, computed as geometric mean of the two horizontal components, at three recording stations (AQK, AQU and AQV).

5. CONCLUSIONS

In this work we have described the main results obtained from 3D numerical simulations of near field earthquake ground motion during the M_W 6.3 2009 L'Aquila earthquake through a high performance spectral element method.
Deterministic numerical simulations were carried out up to frequencies of about 2.5 Hz including a 3D model of the Aterno valley, based on the results of the seismic microzonation campaign performed after the earthquake, and the kinematic source model proposed by Walters et al. (2009). The frequency limit of 3D numerical simulations is mainly related to insufficient details in the source characterization, as well as in the local geological description. In this study, we have shown that high frequency ground motions, within the range of frequencies that the computational grid can actually propagate, can be realistically reproduced by introducing physics-based stochastic spatial variability of kinematic source parameters, such as rise time, rupture velocity and rake angle.
The 3D simulated waveforms turn out to be in satisfactory agreement with the recorded ground motions close to L'Aquila center (stations AQK and AQU), while larger discrepancies are found along the upper Aterno array (AQG-AQA-AQV), where numerical results underestimate the observed amplitudes. In spite of these local differences, a good agreement is found between the simulated PGV wavefield (up to 2.5 Hz) and the spatial distribution of damage, expressed in terms of macroseismic intensity (MCS) observed after the L'Aquila earthquake.
To encourage the engineering applicability of the simulated waveforms, a hybrid scheme has been applied to generate broadband ground motions, combining the LF (f < 2.5 Hz) waveforms from GeoELSE with the HF (f > 3 Hz) synthetics computed through the stochastic method of Motazedian and Atkinson (2005). Displacement and acceleration response spectra of synthetic broadband ground motions were found to be in good agreement with the observations, especially at the stations close to L'Aquila centre.

AKCNOWLEDGEMENTS
To the major extent, this work has been carried out in the framework of the Italian seismological Project S2 *Development of a dynamical model for seismic hazard assessment at national scale'* within the 2007-09 DPC-INGV research programmes. The authors are very grateful to the Consorzio Interuniversitario Lombardo per L'Elaborazione Automatica (CILEA), in Milan, for allowing the extensive use of the Lagrange cluster and providing technical assistance. The fruitful comments of Marco Stupazzini and Manuela Vanini are also gratefully acknowledged.

REFERENCES

Ameri, G., Massa, M., Bindi, D., D'Alema, E., Gorini, A., Luzi, L., Marzorati, S., Pacor, F., Paolucci, R., Puglia, R., and Smerzini, C. (2009). The 6 April 2009 M_W 6.3 L'Aquila (Central Italy) Earthquake: Strong-motion Observations. *Seismological Research Letters* **80**, 951–966.

Ameri, G., Gallovic, F. and Pacor, F. (2012). Complexity of the M_W6.3 2009 L'Aquila (Central Italy) earthquake: 2. Broadband strong-motion modelling. *Journal of Geophysical Research*, doi:10.1029/2011JB008729 (in press)

Anzidei, M., Boschi, E., Cannelli, V., Devoti, R., Esposito, A., Galvani, A., Melini, D., Pietrantonio, G., adn V. Sepe, F. R., and Serpelloni, E. (2009). Coseismic deformation of the destructive April 6, 2009 L'Aquila earthquake (Central Italy) from GPS data. *Geophysical Research Letters* **36**, L17307.

Atzori, S., Hunstad, I., Chini, M., Salvi, S., Tolomei, C., Bignami, C., Stramondo, S., Trasatti, E., Antonioli, A., and Boschi, E. (2009). Finite fault inversion of DinSAR coseismic displacement of the 2009 L'Aquila earthquake (central Italy). *Geophysical Research Letters* **36**, L15305.

Bielak, J., Graves, R. W., Olsen, K. B., Taborda, R., Ram´ırez-Guzm´an, L., Day, S. M., Ely, G. P., Roten, D., Jordan, T. H., Maechling, P. J., Urbanic, J., Cui, Y., and Juve, G. (2010). The ShakeOut earthquake scenario: verification of three simulation sets. *Geophysical Journal International* **180:1**, 375–404.

Blumetti, A. M., Filippo, M. D., Zaffiro, P., Marsan, P., and Toro, B. (2002). Seismic hazard of the city of L'Aquila (Abruzzo — Central Italy): new data from geological, morphotectonic and gravity prospecting analysis. *Studi Geologici Camerti* **1**, 7–18.

Boore, D. (2003). Simulation of Ground Motion Using the Stochastic Method. *Pure and Applied Geophysics* **160:3**, 635–676.

Chiarabba, C., Amato, A., Anselmi, M., Baccheschi, P., Bianchi, I., Cattaneo, M., Cecere, G., Chiaraluce, L., Ciaccio, M., Gori, P. D., Luca, G. D., Bona, M. D., Stefano, R. D., Faenza, L., Govoni, A., Improta, L., Lucente, F., Margheriti, A. M. L., Mele, F., Michelini, A., Monachesi, G., Moretti, M., Pastori, M., Piana Agostinetti, N., Piccinini, D., Roseilli, P., Seccia, D., and Valoroso, L. (2009). The 2009 L'Aquila (Central Italy) M_W6.3 earthquake: Main shock and aftershocks. *Geophysical Research Letters* **36**, L18308.

Cirella, A., Piatanesi, A., Cocco, M., Tinti, E., Scognamiglio, L., Michelini, A., Lomax, A., and Boschi, E. (2009). Rupture history of the 2009 L'Aquila (Italy) earthquake from non-linear joint inversion of strong motion and GPS data. *Geophysical Research Letters* **36**, L19304.

Day, S.M., Graves, R., Bielak, J., Dreger, D., Larsen, S., Olsen, K.B., Pitarka, A., and Ramirez-Guzman, L. (2008). Model for basin effects on long-period response spectra in Southern California. *Earthquake Spectra* **24:1**, 257–277

DBMI Working Group (2009). Database Macrosismico Italiano. Technical report, Istituto Nazionale di Geofisica e Vulcanologia (INGV). http://emidius.mi.ingv.it/DBMI08/

Faccioli, E., Maggio, F., Paolucci, R., and Quarteroni, A. (1997). 2D and 3D elastic wave propagation by a pseudo-spectral domain decomposition method. *Journal of Seismology* **1:3**, 237–251.

Galli, P. and Camassi, R. (2009). Report on the effects of the Aquilano earthquake of 6 April 2009, by QUEST, Quick Earthquake Survey Team. Technical report, Istituto Nazionale di Geofisica e Vulcanologia (INGV). Available at http://emidius.mi.ingv.it/DBMI08/aquilano/.

Graves, R. W. and Pitarka, A. (2010). Broadband Ground-Motion Simulation Using a Hybrid Approach. *Bulletin of Seismological Society of America* **100:5A**, 2095–2123.

Graves, R., Jordan, T., Callaghan, S., Deelman, E., Field, E., Juve, G., Kesselman, C., Maechling, P., Mehta, G., Milner, K., Okaya, D., Small, P., and Vahi, K. (2010). CyberShake: A Physics-Based Seismic Hazard Model for Southern California. *Pure and Applied Geophysics* **168**, 367-381

Herrero, A. and Bernard, P. (1994). A kinematic self-similar rupture process for earthquakes. *Bulletin of the Seismological Society of America* **84**, 1216–1229.

Jones, L. M., Bernknopf, R., Cox, D., Goltz, J., Hudnut, K., Mileti, D., Perry, S., Ponti, D., Porter, K., Reichle, M., Seligson, H., Shoaf, K., Treiman, J., and Wein, A. (2008) The ShakeOut Scenario. Technical Report USGS-R1150, U.S. Geological Survey and California Geological Survey.

Mai, P. and Beroza, G. (2002). A spatial random field model to characterize complexity in earthquake slip. *Journal of Geophysical Research* **107:B11**, 2308–2329.

Mai, P. M., Imperatori, W., and Olsen, K. B. (2010). Hybrid Broadband Ground-Motion Simulations: Combining Long-Period Deterministic Synthetics with High-Frequency Multiple S-to-S Backscattering. *Bulletin of Seismological Society of America* **100:5A**, 2124–2142.

Milana, G., Azzara, R., Bertrand, E., Bordoni, P., Cara, F., Cogliano, R., Cultrera, G., Di Giulio, G., Duval, A., Fodarella, A., Marcucci, S., Pucillo, S., R´egnier, J., and Riccio, G. (2011). The contribution of seismic data in microzonation studies for downtown L'Aquila. *Bulletin of Earthquake Engineering* **9:3**, 741–759.

Motazedian, D. and Atkinson, G. M. (2005). Stochastic Finite-Fault Modeling Based on a Dynamic Corner Frequency. *Bulletin of the Seismological Society of America* **95:3**, 995–1010.

MS-AQ Work Group (2010) Microzonazione sismica per la ricostruzione dell'area aquilana. Technical report, Department of Civil Protection, Italy.

Smerzini, C. and Villani, M. (2012). Broadband numerical simulations in complex near field geological configurations: the case of the M_W 6.3 2009 L'Aquila earthquake. *Bulletin of the Seismological Society of America*, submitted for publication.

Walters, R. J., Elliott, J., D'Agostino, N., England, P., Hunstad, I., Jackson, J., Parsons, B., Phillips, R., and Roberts, G. (2009). The 2009 L'Aquila earthquake (Central Italy): A source mechanism and implications for seismic hazard. *Geophysical Research Letters* **36**, L17312.